

Models of permeability contrasts in subduction zone mélange: Implications for gradients in fluid fluxes, Syros and Tinos Islands, Greece

Jay J. Ague

Department of Geology and Geophysics, Yale University, P.O. Box 208109, New Haven, CT 06520-8109, USA

Accepted 18 August 2006

Editor: S.L. Goldstein

Abstract

Geological and geochemical evidence from previous studies suggest limited fluid flow through the interiors of many blocks of subducted oceanic crust within meta-ultramafic or metasedimentary mélange matrix on the islands of Syros and Tinos, Cyclades, Greece. This finding is provocative because metamorphic devolatilization of igneous and sedimentary rocks during subduction should have liberated substantial volumes of fluid. In an effort to address this problem, two-dimensional numerical models incorporating permeability anisotropy and devolatilization are used to investigate spatial patterns of steady-state fluid flow through subduction zone mélange under high-pressure/low-temperature (HP/LT) conditions. The modeling shows that as the permeability of the mélange blocks decreases relative to the mélange matrix, more flow is diverted around the blocks into the matrix. The ratio of the maximum flux (in matrix) relative to the minimum flux (in blocks) increases with the permeability contrast between the matrix and the less permeable blocks. Order-of-magnitude variations in permeability produce order-of-magnitude spatial variations in fluid fluxes between block interiors and surrounding matrix; flux variations of a factor of 10 or more can be present over very short length scales (as little as meter scale). The largest fluxes are produced in the matrix adjacent to block margins lying sub-parallel to regional foliation and flow direction. Fluid–rock reaction on block margins would be greatest in these areas, leading to asymmetrical distributions of reaction progress around blocks (illustrated herein by field mapping of a mélange block on Syros). However, syn-metamorphic deformation can rotate blocks and strip off reaction zones at their margins, so it is likely that reaction zone asymmetries are commonly disrupted in nature. The inferred absence of strong fluid–rock reaction within mélange blocks on Syros and Tinos could reflect low permeabilities in block interiors which acted to divert flow into mélange matrix. Consequently, fluxes of subduction zone fluids through the mélange matrix could have easily been very large, while low permeabilities shielded block interiors from the regional flow to varying degrees.

© 2006 Elsevier B.V. All rights reserved.

Keywords: Subduction; Mélange; Fluid flow; Modeling; Greece; Cyclades

1. Introduction

Subduction of sediment and hydrothermally altered oceanic crust and mantle is the primary means by which

reactive volatiles including H₂O and CO₂ are returned to the deep Earth. Fluids released during prograde heating may migrate subvertically upward into the overlying accretionary prism or mantle wedge, and also migrate parallel to the slab through the subducted crust itself or along the basal décollement. Modeling results suggest

E-mail address: jay.ague@yale.edu.

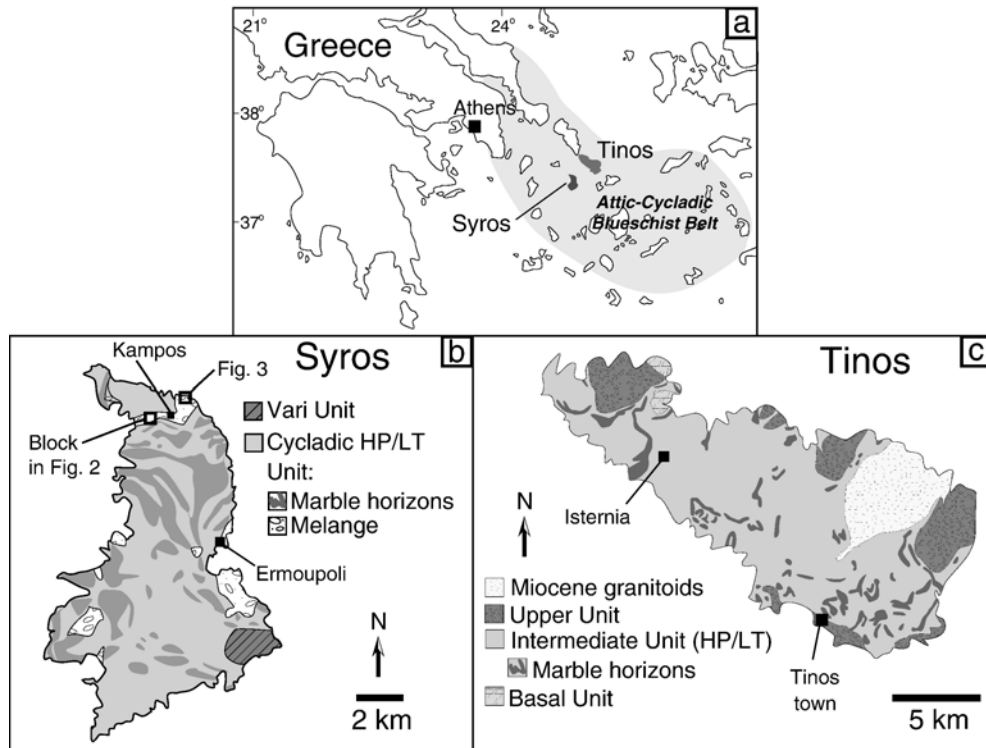


Fig. 1. Location and simplified geologic maps. Modified after Melidonis (1980), Bröcker et al. (1993) and Bröcker and Enders (2001). (a) Map of Greece illustrating positions of Syros and Tinos within the Attic–Cycladic blueschist belt. (b) Geology of Syros, showing main Cycladic volcano-sedimentary HP/LT unit including marbles and mélangé, structurally overlying Vari gneiss (not HP/LT), and localities for Figs. 2 and 3. (c) Geology of Tinos, illustrating main volcano-sedimentary HP/LT unit (Intermediate Unit) which includes marble horizons and mélangé blocks of blueschist, eclogite, meta-gabbro, and jadeitite.

that large-scale fluid fluxes are realized during subduction zone devolatilization (cf. Kerrick and Connolly, 2001a,b; Gorman et al., 2006), and may be as great as $\sim 6000 \text{ m}^3 \text{ m}^{-2} \text{ My}^{-1}$ in the mantle hanging wall (Peacock, 1990). Field studies of stable isotope systematics (e.g., Bebout and Barton, 1989, 1993) and trace element mobility (e.g., Sorensen and Grossman, 1989) provide strong evidence for regional, km-scale fluid migration during Mesozoic subduction in the Cordillera (California, USA). Field and theoretical studies also suggest that large-scale fluid flow may transport significant mass of “non-volatile” elements including Si, Al, and alkali and alkaline earth metals, producing metasomatic alteration features such as regional vein systems and silicification of the mantle wedge (e.g., Bebout and Barton, 1989, 1993; Manning, 1997; Bebout and Barton, 2002; King et al., 2003).

In contrast, mounting evidence from the Cycladic Archipelago (Greece) and the Alps indicates that subduction and high-pressure/low-temperature (HP/LT) metamorphism during Alpine orogenesis may have involved limited, perhaps highly channelized

fluid flow and fluid–rock interaction (e.g., Philippot and Selverstone, 1991; Selverstone et al., 1992; Bröcker et al., 1993; Getty and Selverstone, 1994; Barnicoat and Cartwright, 1995; Ganor et al., 1996; Putlitz et al., 2000). The possible highly limited nature of the flow was highlighted recently by Putlitz et al. (2000) who,

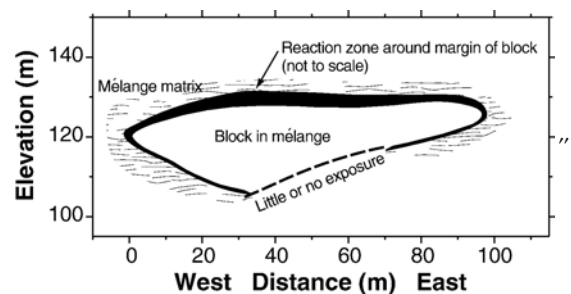


Fig. 2. Field map of layered mélangé block at locality illustrated in Fig. 1b. Block consists primarily of interlayered blueschist and eclogite, and includes some retrogressed rocks originally rich in jadeite. It may represent a metamorphosed sequence of mafic and more felsic volcanic rocks. Reaction rind (black) thickness at contact with ultramafic matrix varies from about 5–15 cm to as much as 1.6 m.

based on O and H isotope studies of metabasalts and metagabbros in the Cyclades, found no evidence favoring regional fluid release and flow during HP/LT metamorphism of the subducted oceanic crust. Moreover, their data gives no indication that significant metamorphic infiltration occurred during earlier, lower-pressure stages of subduction. This result is particularly thought-provoking because clays, serpentine, and carbonate minerals in the precursor sediments and hydrothermally altered igneous rocks should have released abundant volatiles during prograde HP/LT metamorphism. One possible explanation for the apparent absence of strong fluid–rock interaction in some rock types is channelization of metamorphic fluids leading to marked spatial variations in fluid fluxes. Breeding et al. (2004) concluded that significant fluid flow occurred through mélangé on the island of Syros (Greece) and drove considerable fluid–rock interaction and metasomatism on the rims of metasedimentary rock packages in contact with ultramafic mélangé matrix. The interiors of the packages, however, could have undergone much less fluid infiltration. This paper uses numerical models to examine the possible impact of permeability variations on patterns of fluid flow in subduction zone mélangé. Exposures of HP/LT rocks on

the Cycladic islands of Tinos and Syros (Greece) provide geological context for the models (Fig. 1). Breeding et al. (2003) examined how permeability variations could have led to the preservation of HP/LT mineral assemblages during greenschist facies retrograde fluid infiltration on Tinos; the results of the present study are relevant for prograde settings as well as retrograde, exhumation settings. In this paper, rock permeability that is uniform and does not vary with direction is termed isotropic, whereas permeability that varies with direction is termed anisotropic. Differences in permeability between rock types are referred to in a general way as permeability contrasts or permeability heterogeneities; the rock types can be isotropic or anisotropic.

2. Geologic setting

Regional HP/LT blueschist and eclogite facies metamorphism in the Attic–Cycladic Crystalline Belt of the Aegean region occurred during subduction of the Apulian microplate beneath Eurasia in the Alpine orogeny (cf. Bonneau, 1984). The timing remains controversial; Bröcker and Enders (1999) argue for Cretaceous–Tertiary metamorphism whereas Tomaschek et al. (2003) concluded that it occurred during the Eocene. HP/LT metamorphic conditions were in the range of 1.5 ± 0.3 GPa and ~ 500 – 550 °C (Schliestedt et al., 1987; Avigad et al., 1988; Okrusch and Bröcker, 1990; Bröcker et al., 1993; Matthews, 1994; Putlitz et al., 2000); the highest reported pressures are ~ 1.8 – 2.0 GPa (Trotet et al., 2001a,b). HP/LT mélangé sequences on Syros and Tinos are characterized by blocks of blueschist, eclogite, meta-gabbro, jadeitite, and serpentinite set in a foliated matrix of serpentinitic or metasedimentary rock (Dixon and Ridley, 1987; Brady et al., 2000; Bröcker and Enders, 2001). In many areas (e.g., northwestern Syros), syn-subduction deformation juxtaposed the mélangé with surrounding metasedimentary rocks (cf. Dixon and Ridley, 1987; Okrusch and Bröcker, 1990; Breeding et al., 2004). The mélangé is generally interpreted to represent a highly deformed and dismembered ophiolite sequence, but mélangé origins, whether tectonic, sedimentary, or some combination, remain controversial (cf. Altherr and Seidel, 1977; Höpfer and Schumacher, 1977; Bonneau et al., 1980; Dixon and Ridley, 1987; Bröcker and Enders, 1999, 2001).

The classic observations of Dixon and Ridley (1987) documented metasomatic exchange of non-volatile elements at lithologic contacts between mélangé blocks and surrounding serpentinitic matrix on Syros. Reaction rinds rich in omphacite, glaucophane, and/or chlorite ranging in

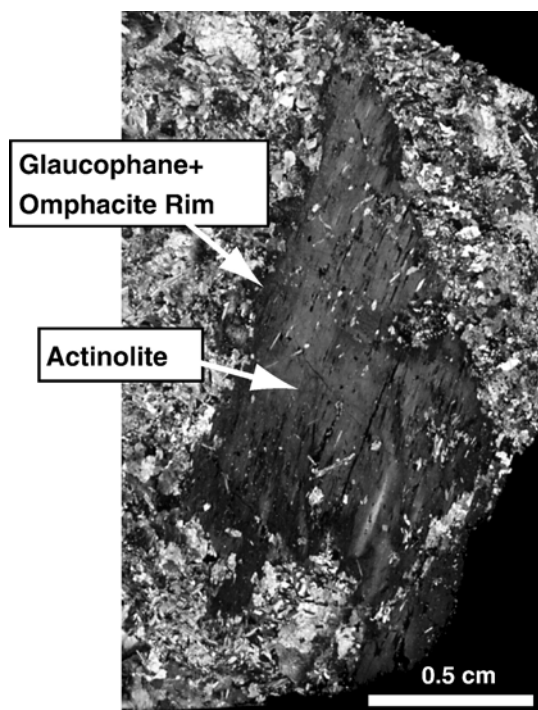


Fig. 3. Thin section photomicrograph illustrating large relic actinolite crystal rimmed by glaucophane and omphacite in metagabbro (crossed polarizers; see Fig. 1 for sample location). Matrix consists mostly of clinozoisite, quartz, and white mica.

thickness from the cm scale to m scale are common on block margins (cf. Dixon and Ridley, 1987; Bröcker and Enders, 2001; Marschall et al., 2006). These reaction features resemble those documented in *mélange* in California, and indicate substantial fluid–rock interaction on the rims of blocks (e.g., Bebout and Barton, 2002). Fluid-driven metasomatism also produced glaucophane-rich alteration zones up to 2.5 m thick in metasediments along contacts with meta-ultramafic *mélange* matrix (Breeding et al., 2004). Asymmetric reaction rims on the margins of blocks are evident at several localities on Syros (Fig. 2). Where large, consistent asymmetries are exposed, the rims are thickest sub-parallel to the dominant foliation in the surround *mélange* matrix. The thickest part of the reaction zone in Fig. 2 is ~1.6 m thick, and it thins by a factor of 10 or more to ~5–15 cm elsewhere. The margins of this and most other blocks have clearly undergone strong metasomatism (Dixon and Ridley, 1987), but isotopic evidence from block interiors suggests much more limited metamorphic fluid–rock interaction (Putlitz et al., 2000). It is important to point out, however, that fractures/veins in the blocks do occur and, on Syros, they are commonly surrounded by glaucophane and/or omphacite-rich alteration zones or “selvages” that resemble mineralogically the reaction zones on block rims. These relations indicate that significant quantities of *mélange* fluids could penetrate the blocks along fractures to promote infiltration-driven reactions.

The *mélange* matrix on Tinos appears to be mostly metasedimentary but also includes metavolcanic rocks. Ultramafic matrix and in-situ reaction rinds on blocks have not been observed (Bröcker and Enders, 2001). The lack of reaction rinds may be due to the absence of serpentinite matrix, but observations could be complicated by outcrop limitations (block–matrix contacts are rarely exposed on Tinos) and by the extensive retrograde metamorphism that affected most of the HP/LT rocks on Tinos (cf. Bröcker et al., 1993). Interestingly, nearly monomineralic actinolite, glaucophanite, and omphacite rocks similar to those found in reaction rinds on Syros occur as float or small isolated boulders on Tinos. However, it remains to be documented whether or not these float/boulder assemblages formed as a result of block–ultramafic matrix interactions. Bröcker and Enders (2001) documented unusual bulk compositions strongly enriched in many important minor and trace elements (e.g., Ti, Zr, Y) for some blocks on both Tinos and Syros. They interpreted the trace element signatures to be the result of HP/LT metasomatic alteration; if so, these unusual blocks underwent considerably more fluid infiltration than those studied by Putlitz et al. (2000).

The predominantly metaigneous blueschist, eclogite, and meta-gabbro block interiors on Syros and Tinos are generally massive, are relatively poor in sheet silicates, and are often weakly foliated. These characteristics almost certainly limited their permeability relative to the strongly-foliated, sheet silicate-rich *mélange* matrix. The blocks were also much more competent than the matrix during deformation, which probably restricted the amount of deformation-enhanced porosity and permeability that could develop within them. The degree of recrystallization within blocks was remarkably small in some cases; for example, the interiors of large meta-gabbro blocks (Figs. 1 and 3) can retain actinolite (cf. Ridley and Dixon, 1984; Putlitz et al., 2000) that is presumably a relic from seafloor alteration or lower-temperature stages of the metamorphism.

The sources of the fluids within the *mélange* remain to be fully characterized. Possibilities include fluid derived from: (1) devolatilization of surrounding metasedimentary and metaigneous rocks that was focused into the *mélange*; (2) dehydration of *mélange* matrix; and (3) individual *mélange* blocks that dehydrated and contributed fluid to the overall flow within the matrix.

Putlitz et al. (2000) also found no conclusive evidence favoring large HP/LT fluid fluxes through metabasic rocks on the neighboring island of Sifnos. These rocks crop out as lenses and larger masses of blueschist and eclogite within a dominantly metasedimentary rock package (cf. Trotet et al., 2001a,b), but are traditionally not mapped as part of a *mélange* sequence. However, strong deformation could have obscured geologic relations, and it is noteworthy that the two main tectonic units on the island are separated by a low-angle fault containing serpentinite lenses (cf. Trotet et al., 2001a,b).

3. Methods

This study examines steady-state Darcian fluid flow through a two-dimensional section of *mélange* 100 m long. The width of the *mélange* varies in the field; 60 m was used based on field relations at the site depicted in Fig. 2. The model *mélange* includes a variety of randomly-placed, circular and elliptical *mélange* blocks of varying size comprising 25% of the flow region. An infinite number of block configurations are possible; the one used here is based on representative field relations and illustrates some important basic physics of flow in a heterogeneous *mélange* system. Model fluid fluxes are insufficient to transport large amounts of heat by advection and, thus, temperature (T) was held constant (see below). This constraint would not be applicable if, for example, fluid fluxes were larger or if significant heat was consumed by

rapidly-proceeding dehydration reactions. Conservation of mass is given by (e.g., Bear, 1972):

$$\frac{\partial(\rho_f \phi)}{\partial t} = 0 = -\nabla \cdot (\rho_f \mathbf{q}) + S_f \quad (1)$$

in which ρ_f is the fluid density, ϕ is porosity, \mathbf{q} is the fluid flux vector, and S_f is the fluid source term. The fluid flux is given by Darcy's law:

$$\mathbf{q} = -\frac{\tilde{k}}{\mu} \cdot (\nabla P_f + \rho_f g \nabla Z) \quad (2)$$

where \tilde{k} is the intrinsic permeability tensor, μ is the fluid viscosity, P_f is fluid pressure, g is the acceleration of gravity expressed as a constant, and Z is a vertical reference coordinate that increases upward. Viscosity was calculated using code from the HYDROTHERM program (Hayba and Ingebritsen, 1994). The matrix foliation is assumed to be the primary control on permeability anisotropy and is taken to be parallel to the z coordinate axis (vertical). The maximum and minimum permeabilities in the matrix are parallel to the z and x coordinate axes, respectively, such that the permeability tensor is:

$$\tilde{k} = \begin{pmatrix} k_{xx} & 0 \\ 0 & k_{zz} \end{pmatrix} \quad (3)$$

Permeabilities in the range 10^{-18} to 10^{-20} m² were investigated, compatible with the results of Ingebritsen and Manning (1999) and Manning and Ingebritsen (1999). Metamorphic foliations defined by platy minerals such as serpentine or phengite almost certainly produced permeability anisotropy in the mélange matrix. Huenges et al. (1997) found that mean permeability parallel to foliation can be as much as a factor of ~ 10 greater than perpendicular to it. Numerous field-based studies also document that flow is generally greatest parallel to foliation and layering (cf. Rye et al., 1976; Rumble and Spear, 1983; Ganor et al., 1989; Baker, 1990; Oliver et al., 1990; Ferry, 1994; Ague, 2003).

The fluid is weakly compressible and, for the limited range of pressures examined here, is adequately represented by:

$$\beta_f = \frac{1}{\rho_f} \left(\frac{\partial \rho_f}{\partial P_f} \right)_T \quad (4)$$

in which β_f is the fluid compressibility (cf. Bear, 1972; Walder and Nur, 1984). The rate of fluid release by dehydration of mélange blocks was estimated using (Hanson, 1997):

$$S_f = \frac{\chi_f \rho_{rk}}{\Delta T} \frac{dT}{dt} \quad (5)$$

in which χ_f is the mass fraction of fluid released, ρ_{rk} is the rock density, and ΔT is the temperature interval over which the fluid is released. The models use representative values of $\chi_f = 0.05$ kg (H₂O) kg⁻¹ (rock), $\rho_{rk} = 3000$ kg m⁻³, and $\Delta T = 600$ °C. If the rock is subducted at a rate of 10^{-2} m year⁻¹ along a geothermal gradient of 10 °C km⁻¹, then dT/dt is 10^{-4} °C year⁻¹. Increasing the subduction rate to 5×10^{-2} yields $dT/dt = 5 \times 10^{-4}$ °C year⁻¹. Either value yields nearly identical results in the modeling, so only results for 10^{-4} °C year⁻¹ are shown. Furthermore, simulations in which blocks and matrix dehydrate simultaneously (not illustrated) have flow systematics that are essentially the same as those shown herein. Note that because T is constant in the models, Eq (5) is not strictly applicable. However, the flow region comes to steady state in a short period of model time (year to decade time scales) relative to the heating rate, so the small increases in T required for dehydration according to Eq. (5) have a negligible impact on the “snapshots” of flow behavior computed in the models. The impact of the advective component of heat transport due to fluid flow can be approximated using the following simplified expression that follows directly from conservation of energy (e.g., Ague, 2000):

$$\frac{\partial T}{\partial t} \approx q_z \frac{\rho_f c_{P,f}}{\rho_{rk} c_{P,rk}} \frac{\partial T}{\partial z} \quad (6)$$

in which q_z is the average flux in the z direction and $c_{P,f}$ and $c_{P,rk}$ are the heat capacities of fluid and rock, respectively. For a geothermal gradient of 10 °C km⁻¹ and representative heat capacities (Brady, 1988) and model fluxes (10^{-3} to 5×10^{-3} m³ m⁻² year⁻¹; see below), $\partial T/\partial t$ is in the range of 10^{-5} to 10^{-4} °C year⁻¹, small enough to be neglected for the simulations herein.

Porosity was set to a constant value of 10^{-3} throughout the domain (cf. Ague, 2000). Different values would increase or decrease fluxes, but the general patterns of flow around mélange blocks would be similar to those shown. Increases in fluid pressure can increase porosity and vice versa, and can be treated using a “pore compressibility” term (cf. Walder and Nur, 1984; Ague et al., 1998). Values of pore compressibility for rocks are not well-known, but are small and are probably $< 5 \times 10^{-9}$ Pa⁻¹ (Wong et al., 1997). For the present study, this translates into negligible variation in porosity given that fluid pressure varies by $\lesssim 10^6$ Pa at any given elevation across the flow region. Of course, chemical reactions can produce considerable irreversible changes in porosity as well as permeability (cf. Ague et al., 1998; Balashov and Yardley, 1998; Bolton et al., 1999); treatment of these phenomena will require detailed

models of subduction zone devolatilization and metasomatic reactions.

T and P_f were initially set to 550 °C and 1.5 GPa in the base ($z=0$) of the flow region. T was then initialized throughout the domain using a geothermal gradient of 10 °C km⁻¹, and P_f was initialized using a lithostatic gradient (cf. Hanson, 1997). Once T and initial P_f were set, β_f was computed throughout the flow domain using the CORK equation of state for ρ_f (Holland and Powell, 1991). “No-flow” (or “symmetrical”) boundary conditions were employed at $x=0$ m and $x=60$ m. P_f was held constant at $z=0$ m and $z=100$ m, although it is important to note that P_f and gradients in P_f within the flow region could freely evolve to steady state. A uniform, time-invariant flux boundary condition at $z=0$ m yields similar results (not shown). Many other initial and boundary condition configurations are possible, but the general systematics of flow around mélange blocks illustrated here would be little affected. Finite-difference numerical methods were used to solve for fluid flow. Additional discussion of solution procedures and model verification can be found in Ague (1998, 2000) and Ague and Rye (1999). It is worth noting in this regard that fluid mass fluxes into and out of steady-state systems with no fluid sinks/sources should match, providing a powerful test of numerical algorithms. Test simulations with no dehydration show that average input and output fluxes are in excellent agreement and differ by less than 0.02%. The time-dependent conservation of mass equation was iterated from the initial condition to steady state. A very fine grid spacing of 0.25 m in both the x and z directions allows imaging of flow variations with high spatial resolution.

4. Results

Flow through the low-permeability mélange blocks is limited, so the flow is directed around them into the higher-permeability matrix (Fig. 4). As a consequence, fluxes are also limited upstream and downstream of the blocks; these “shadow” zones of low flux can extend tens of meters into the matrix and affect fluxes in and around neighboring blocks. The largest fluxes are concentrated in the matrix at block margins lying sub-parallel to the foliation and overall flow direction, roughly perpendicular to the upstream and downstream ends of the blocks (Fig. 4). The range of fluid fluxes is primarily dependent on the permeability contrasts between blocks and matrix, although other factors including the number of blocks and their sizes and shapes also play a role. As shown in Fig. 5, the ratio of the maximum to minimum flux increases strongly as the

permeability of the blocks decreases and more and more fluid is diverted out into the matrix. Importantly, the high spatial resolution grid used in the models predicts that this flow focusing can lead to large flux variations of an order of magnitude or more over meter scale distances (Figs. 4b,c and 6). Furthermore, the diversion of flow around blocks means that fluxes can vary widely from place to place within the matrix, even though its permeability structure is the same throughout the domain (Fig. 6). In nature, it is possible that the reaction rinds could be more permeable than the block interiors, leading to increased flow through the margins of the blocks as metasomatism proceeds. Flow systematics for an isotropic matrix are illustrated in Figs. 4d and 7b. Results are similar in many respects to the anisotropic cases, but the larger flux areas around blocks tend to be wider as flow is not constrained by a matrix foliation (Figs. 4d and 7).

The models predict limited fluid influx into the low-permeability blocks, but fractures in the blocks could elevate permeability and allow fluid infiltration. A simple illustration of this phenomenon is shown in Fig. 4e, in which the largest model block is bisected by a 0.25 m wide, high-permeability zone representing a fracture. Considerable fluid flow is focused into the model fracture, demonstrating a possible mechanism by which fluids could gain access to the interior of low-permeability blocks (Figs. 4e and 6b). It is possible that fracture networks facilitated the metasomatic fluid infiltration that produced the unusual trace element signatures documented by Bröcker and Enders (2001) within some blocks. It is also possible that these blocks were more permeable than others, such that infiltration-driven metasomatism occurred more pervasively within them. Further work is needed to determine the nature and extent of fracture networks and their impact on fluid–rock reactions within blocks.

The models include prograde dehydration of blocks, but it should be noted that the general diversion of flow around low-permeability blocks would be similar for exhumation settings in which there was flow through the matrix but no fluid production within blocks. Flow during exhumation and decompression was considerable in many parts of the Cyclades (cf. Bröcker et al., 1993; Marschall et al., 2006).

5. Discussion and conclusions

The modeling illustrates how fluid flow in mélange can be diverted around low-permeability matrix blocks. Fluxes are concentrated in the matrix around block margins sub-parallel to matrix foliation and the overall

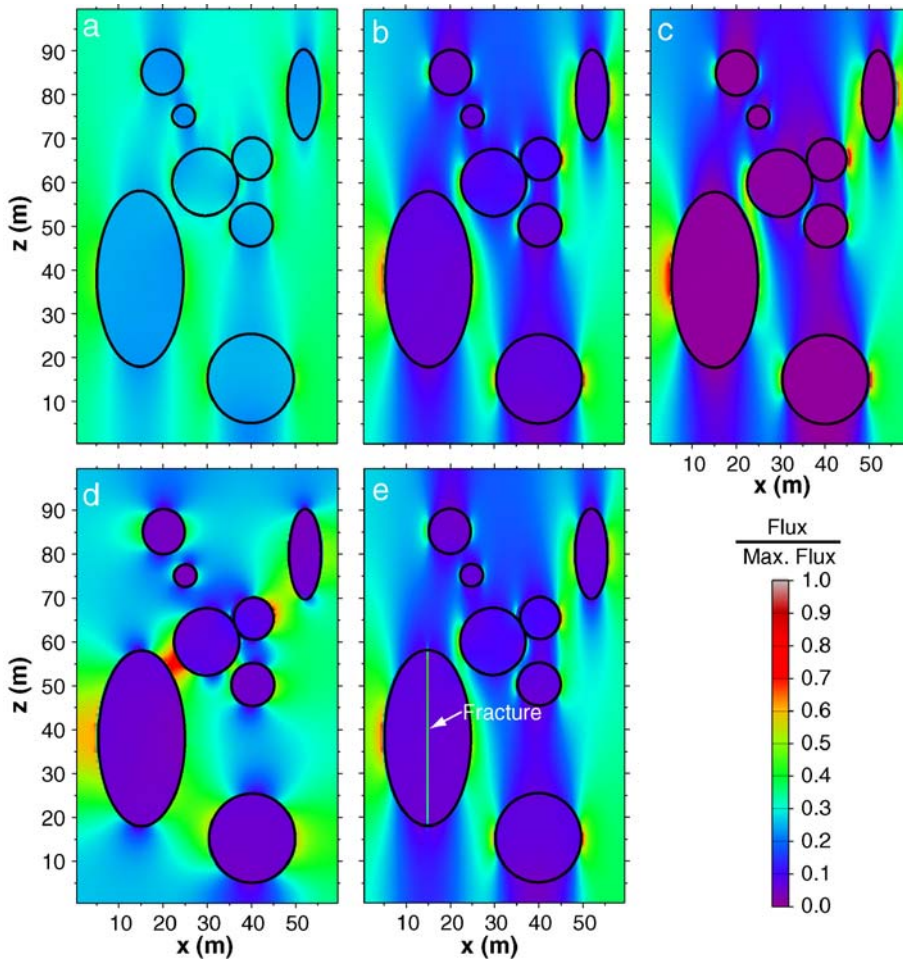


Fig. 4. Model fluid flow results (see text for discussion). For all parts except (d), matrix has permeability of 10^{-18} m^2 parallel to z , and 10^{-19} m^2 parallel to x ; blocks are isotropic in all cases. Flux contours normalized to maximum value of $1.4 \times 10^{-2} \text{ m}^3 \text{ m}^{-2} \text{ year}^{-1}$ attained in part (c). Average fluxes typically in the range 10^{-3} to $5 \times 10^{-3} \text{ m}^3 \text{ m}^{-2} \text{ year}^{-1}$. (a) Permeability of blocks ($5 \times 10^{-19} \text{ m}^2$) a factor of 2 less than maximum permeability in matrix. (b) Permeability of blocks (10^{-19} m^2) a factor of 10 less than maximum permeability in matrix. (c) Permeability of blocks (10^{-20} m^2) a factor of 100 less than maximum permeability in matrix. (d) Isotropic matrix and blocks with permeabilities of 10^{-18} m^2 and 10^{-19} m^2 , respectively. (e) Like part (b), except that largest block is cut by a model high-permeability fracture that has the same permeability as the matrix.

fluid flow direction. The ratio of maximum flux (in matrix)/minimum flux (in blocks) increases log linearly with the ratio of maximum permeability (in matrix)/minimum permeability (in blocks). Consequently, order-of-magnitude variations in permeability are needed to produce order-of-magnitude spatial variations in fluid fluxes (Figs. 4 and 5). An important next step for future work will be to better constrain the permeability tensor in mélange materials using laboratory measurements. The model flow patterns provide a testable hypothesis to account for the stable isotope systematics observed by Putlitz et al. (2000) in mélange blocks on Syros and Tinos. If the blocks had average permeabilities a factor of ~ 10 or smaller than the maximum permeability of the

matrix, then metamorphic fluid infiltration into the blocks could have been limited, thus preserving the oxygen isotope signatures of basaltic and gabbroic oceanic crust within the blocks. The time-integrated fluid flux (q_{TI}) within the blocks could thus have been dominated by their internal dehydration. For a spherical block, it is easily shown that the q_{TI} at the block surface can be estimated by:

$$q_{\text{TI}} = \frac{r\chi_f\rho_{\text{rk}}}{3\rho_f} \quad (7)$$

where r is the radius of the block. Given that $3\rho_f$ is roughly equivalent to ρ_{rk} , the approximation for q_{TI} simplifies to: $r\chi_f$. For example, for complete dehydration

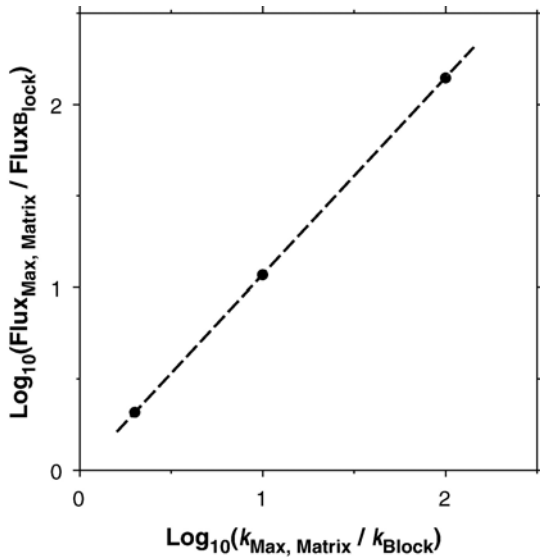


Fig. 5. Relations between fluid flux and permeability (k). \log_{10} (maximum fluid flux in matrix)/(minimum fluid flux in block) as a function of \log_{10} (maximum permeability in matrix)/(permeability of blocks). Note that ratio of maximum/minimum fluid flux scales with the permeability ratio. Dots represent results for a range of model runs. Minimum flux assessed in center of large elliptical block in lower left part of flow domain (Fig. 4).

of a block with $r=10$ m and $\chi_f=0.05$, the estimated q_{TI} is $\sim 0.5 \text{ m}^3 \text{ (fluid) m}^{-2} \text{ (rock)}$. Such fluxes are small and insufficient to strongly modify gabbroic and basaltic ocean floor isotopic signatures (cf. Dipple and Ferry, 1992). As noted above, the HP/LT rocks on Sifnos studied by Putlitz et al. (2000) may not be part of a mélangé. Nonetheless, fluid flow through the metasediments could

have been diverted around the blueschist and eclogite bodies in much the same way as depicted in Fig. 4. It is also possible that most of the rock types on Sifnos were characterized by very low permeability which diverted flow around the entire rock package and strongly limited flow within it (cf. Ganor et al., 1989, 1991).

The q_{TI} needed for oxygen isotopic homogenization due to fluid advection through blocks can be estimated. For local fluid–rock isotopic equilibrium, $d=v\phi tK_v$ in which K_v is the fluid/solid partition coefficient by volume (0.6 for oxygen), v is the mean pore fluid velocity, and d is the distance of isotopic front propagation (Bickle, 1992; Dipple and Ferry, 1992). Taking $q_{TI}=v\phi t$, it is easily shown that the oxygen isotopic composition of a representative 10 m length scale block would be reset for time-integrated fluid fluxes of $\sim 17 \text{ m}^3 \text{ m}^{-2}$ or greater. For a permeability contrast of 100, the minimum model flux ($v\phi$) through blocks is $\sim 1.4 \times 10^{-4} \text{ m}^3 \text{ m}^{-2} \text{ year}^{-1}$ (Fig. 4c), so the necessary timescale of fluid–rock interaction would be only $\sim 10^5$ years. Timescales would be correspondingly longer for lower block permeabilities or slower rates of fluid flow. It should be emphasized that these calculations carry many uncertainties, such as those on model fluid fluxes. Furthermore, if kinetic factors limited rates of isotopic exchange, then the q_{TI} values needed to reset the isotopic compositions of blocks would be underestimated by the above analysis. Moreover, isotopic transport by diffusion and mechanical dispersion are not accounted for, but these processes would also act to modify the isotopic composition of blocks. Nonetheless, the calculations suggest that the time-integrated fluid

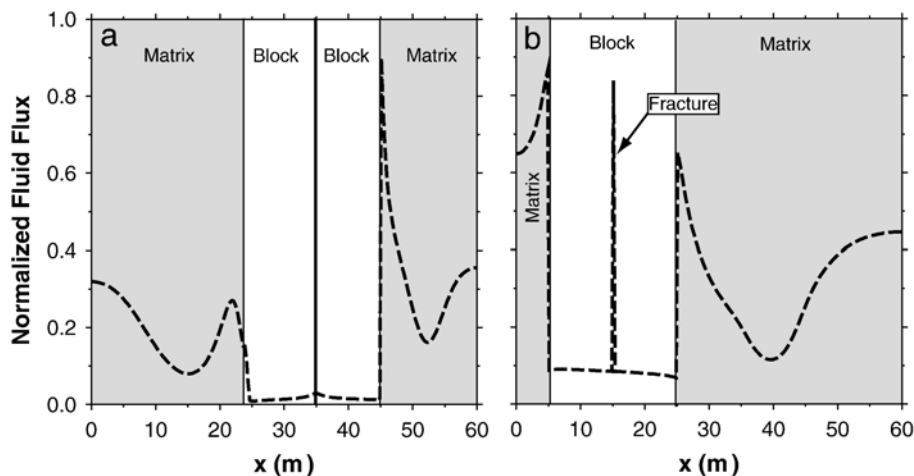


Fig. 6. Normalized fluid fluxes at constant elevations plotted as functions of x . (a) Fluxes at $z=65$ m for model shown in Fig. 4c. Note that largest fluxes are found in matrix on margins of blocks, and that extreme gradients in fluxes can develop over m-scale distances. (b) Fluxes at $z=38$ m for model shown in Fig. 4e. Note large fluxes in matrix on margin of block and within block along model fracture.

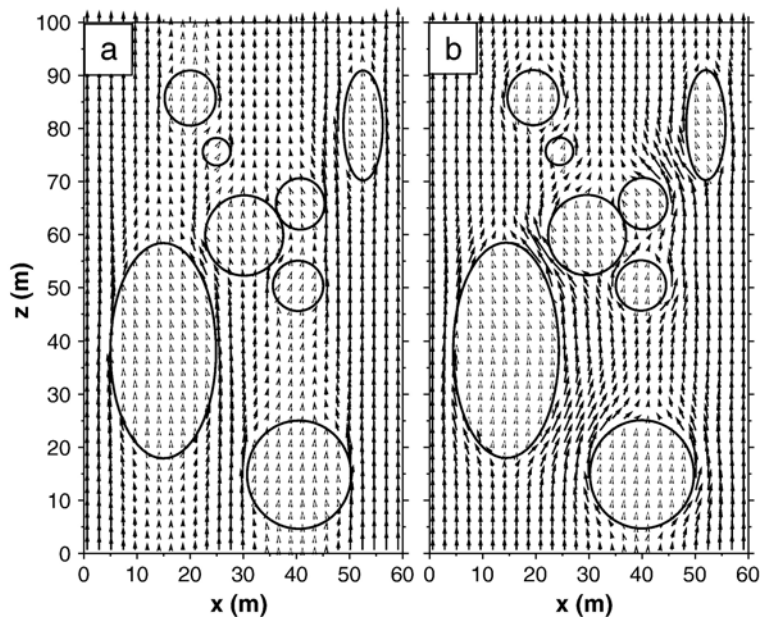


Fig. 7. Example fluid flow vector diagrams. Lengths of arrows scaled to magnitude of fluid flux. Part (a) is for a foliated matrix and corresponds to the contours shown in Fig. 4b, whereas part (b) is for an isotropic matrix and corresponds to Fig. 4d.

fluxes needed to alter the isotopic compositions of blocks would have been relatively small, consistent with the conclusion that blocks had low permeabilities that limited fluid infiltration. Further field-based work aimed at quantifying time-integrated fluid fluxes through blocks and timescales of fluid–rock interaction would provide valuable tests of model results and hypotheses for fluid flow in mélangé zones.

Metasomatic reaction rinds on block margins on Syros indicate that substantial fluid–rock interaction could occur directly at contacts between matrix and blocks within mélangé (cf. Dixon and Ridley, 1987). The modeling predicts that fluid fluxes will be largest around blocks in regions sub-parallel to foliation and flow direction (Fig. 4). Therefore, the most fluid–rock reaction would be expected to occur in these regions, producing the thickest reaction rinds. On the other hand, rinds would be thinnest on the up and downstream sides of the blocks, where fluxes are smaller. These spatial relations provide a potential means to identify paleo-flow directions in the field. Such reaction rind asymmetry is observed for some mélangé blocks (Fig. 2), but not all. The lack of observable, systematic asymmetry on some blocks not only may be due in part to exposure limitations, but is also probably the result of deformation within the mélangé. As shown by Bebout and Barton (2002) the relatively weak metasomatic rind materials can become disaggregated from the mélangé blocks during deformation and incorporated into mélangé

matrix. The mélangé blocks may rotate during deformation as well. Under these deformational conditions, the asymmetry of the rinds would commonly be disrupted. Nonetheless, the general conclusion that significant flow would be diverted around low-permeability blocks holds even if they rotate or undergo deformation. A future challenge will be to model fluid flow in an actively deforming mélangé system.

Reactions driven by the infiltration of fluids equilibrated with ultramafic mélangé matrix into metasedimentary rocks can produce trace element geochemical signatures in fluids consistent with those inferred for metasedimentary contributions to arc magmas (Breeding et al., 2004). Field observations (e.g., Breeding et al., 2004) show that the strongest interactions occur at contacts and along fractures, consistent with the modeling predictions (Figs. 4 and 6). Conceptual and numerical models of transport and fluid–rock reactions in mélangé should account for the large spatial variations in fluid fluxes that occur in systems with strongly varying permeability. Models that assume uniform flow through all blocks and matrix will likely overestimate the amount of fluid–rock reaction that occurs within blocks, leading to biased assessments of the geochemistry of subduction zone fluids. In conclusion, fluxes through mélangé on Syros and Tinos could have been large during subduction, but low permeabilities in block interiors would have forced flow through the mélangé matrix and limited infiltration deep into the blocks. The

formation of high-permeability fractures in blocks, however, could have facilitated varying degrees of HP/LT fluid flow within them.

Acknowledgements

I would like to thank the editors of this special issue for their invitation to submit this work; C.M. Breeding, M. Bröcker, D.E. Wilbur, D.M. Rye, and E.W. Bolton for many thoughtful discussions in the field and laboratory; D.O. Hayba, S.E. Ingebritsen, P.A. Hsieh, and K.L. Kipp for supplying and helping with the computer code for the viscosity calculations; and the Greece Institute of Geology and Mineral Exploration (IGME) for fieldwork permits. The paper was improved considerably by the thoughtful reviews of G.E. Bebout and J.M. Ferry. Support from National Science Foundation grant EAR-0105927 is gratefully acknowledged.

References

- Ague, J.J., 1998. Simple models of coupled fluid infiltration and redox reactions in the crust. *Contrib. Mineral. Petrol.* 132, 180–197.
- Ague, J.J., 2000. Release of CO₂ from carbonate rocks during regional metamorphism of lithologically heterogeneous crust. *Geology* 28, 1123–1126.
- Ague, J.J., 2003. Fluid infiltration and transport of major, minor, and trace elements during regional metamorphism of carbonate rocks, Wepawaug Schist, Connecticut, USA. *Am. J. Sci.* 303, 753–816.
- Ague, J.J., Rye, D.M., 1999. Simple models of CO₂ release from metacarbonates with implications for interpretation of directions and magnitudes of fluid flow in the deep crust. *J. Petrol.* 40, 1443–1462.
- Ague, J.J., Park, J.J., Rye, D.M., 1998. Regional metamorphic dehydration and seismic hazard. *Geophys. Res. Lett.* 25, 4221–4224.
- Altherr, R., Seidel, E., 1977. Speculations on the geodynamic evolution of the Attic–Cycladic crystalline complex during alpidic times. *Proc. Colloq. Geol. Aegean Reg.*, 6th (1), 347–352.
- Avigad, D., Matthews, A., Garfunkel, Z., 1988. The Alpine Evolution of the Cyclades. An Introduction and Excursion Guide to the Geology of the Islands of Sifnos and Tinos. Department of Geology, Institute of Earth Sciences, The Hebrew University of Jerusalem. 66 pp.
- Baker, A.J., 1990. Stable isotopic evidence for fluid–rock interactions in the Ivrea zone, Italy. *J. Petrol.* 31, 243–260.
- Balashov, V.N., Yardley, B.W.D., 1998. Modeling metamorphic fluid flow with reaction–compaction–permeability feedbacks. *Am. J. Sci.* 298, 441–470.
- Barnicoat, A.C., Cartwright, I., 1995. Focused fluid flow during subduction: oxygen isotope data from high-pressure ophiolites of the western Alps. *Earth Planet. Sci. Lett.* 132, 53–61.
- Bear, J., 1972. *Dynamics of Fluids in Porous Media*. Dover, New York. 764 pp.
- Bebout, G.E., Barton, M.D., 1989. Fluid flow and metasomatism in a subduction zone hydrothermal system: Catalina Schist terrane, California. *Geology* 17, 976–980.
- Bebout, G.E., Barton, M.D., 1993. Metasomatism during subduction: products and possible path in the Catalina Schist, California. *Chem. Geol.* 108, 61–91.
- Bebout, G.E., Barton, M.D., 2002. Tectonic and metasomatic mixing in a high-T, subduction-zone mélange — insights into the geochemical evolution of the slab–mantle interface. *Chem. Geol.* 187, 79–106.
- Bickle, M.J., 1992. Transport mechanisms by fluid-flow in metamorphic rocks: oxygen and strontium decoupling in the Trois Seigneurs Massif — a consequence of kinetic dispersion? *Am. J. Sci.* 292, 289–316.
- Bolton, E.W., Lasaga, A.C., Rye, D.M., 1999. Long-term flow/chemistry feedback in a porous medium with heterogeneous permeability: kinetic control of dissolution and precipitation. *Am. J. Sci.* 299, 1–68.
- Bonneau, M., 1984. Correlation of the Hellenide nappes in the south-east Aegean and their tectonic reconstruction. In: Dixon, J.E., Robertson, A.H.F. (Eds.), *The Geological Evolution of the Eastern Mediterranean*. Geological Society Special Publications, vol. 17. Blackwell, Oxford, pp. 517–527.
- Bonneau, M., Blake, M.C., Geysant, J., Kienast, J.R., Lepvrier, C., Maluski, H., Papanikolaou, D., 1980. Sur la signification des roches métamorphiques (schistes bleus) des Cyclades (Héllénides, Grèce). L'exemple de l'île de Syros. *C. R. Acad. Sci., Ser. D* 290, 1463–1466.
- Brady, J.B., 1988. The role of volatiles in the thermal history of metamorphic terranes. *J. Petrol.* 29, 1187–1213.
- Brady, J.B., Shiver, H., Grandy, A., Cheney, J.T., Schumacher, J.C., 2000. Whole-rock geochemistry and metamorphism of blueschist/eclogite facies mafic rocks on Syros, Cyclades, Greece. *Geological Society of America Abstracts with Programs*, vol. 32, p. A152.
- Breeding, C.M., Ague, J.J., Bröcker, M., Bolton, E.W., 2003. Blueschist preservation in a retrograded, high-pressure, low-temperature metamorphic terrane, Tinos, Greece: implications for fluid flow paths in subduction zones. *Geochem., Geophys., Geosyst.* 4, 9002. doi:10.1029/2002GC000380. 11 pp.
- Breeding, C.M., Ague, J.J., Bröcker, M., 2004. Fluid–metasedimentary rock interactions and the chemical composition of arc magmas. *Geology* 32, 1041–1044.
- Bröcker, M., Enders, M., 1999. U–Pb zircon geochronology of unusual eclogite-facies rocks from Syros and Tinos (Cyclades, Greece). *Geol. Mag.* 136, 111–118.
- Bröcker, M., Enders, M., 2001. Unusual bulk-rock compositions in eclogite-facies rocks from Syros and Tinos (Cyclades, Greece): implications for U–Pb zircon geochronology. *Chem. Geol.* 175, 581–603.
- Bröcker, M., Kreuzer, H., Matthews, A., Okrusch, M., 1993. ⁴⁰Ar/³⁹Ar and oxygen isotope studies of polymetamorphism from Tinos Island, Cycladic blueschist belt, Greece. *J. Metamorph. Geol.* 11, 223–240.
- Dipple, G.M., Ferry, J.M., 1992. Fluid flow and stable isotopic alteration in rocks at elevated temperatures with applications to metamorphism. *Geochim. Cosmochim. Acta* 56, 3539–3550.
- Dixon, J.E., Ridley, J.R., 1987. Syros. In: Helgeson, H.C. (Ed.), *Chemical Transport in Metasomatic Processes*. Dordrecht, Reidel, NATO ASI Series. Springer-Verlag, Berlin, pp. 489–501.
- Ferry, J.M., 1994. Overview of the petrologic record of fluid flow during regional metamorphism in northern New England. *Am. J. Sci.* 294, 905–988.
- Ganor, J.A., Matthews, A., Paldor, N., 1989. Constraints on effective diffusivity during oxygen isotope exchange at a marble–schist contact, Sifnos (Cyclades), Greece. *Earth Planet. Sci. Lett.* 94, 208–216.
- Ganor, J.A., Matthews, A., Paldor, N., 1991. Diffusional isotopic exchange across an interlayered marble–schist sequence with an application to Tinos, Cyclades, Greece. *J. Geophys. Res.* 96, 18,073–18,080.

- Ganor, J., Matthews, A., Schliestedt, M., Garfunkel, Z., 1996. Oxygen isotope heterogeneities of metamorphic rocks: an original tectonostratigraphic signature, or an imprint of exotic fluids? A case study of Sifnos and Tinos Islands (Greece). *Eur. J. Mineral.* 8, 719–731.
- Getty, S., Selverstone, J., 1994. Stable isotope and trace element evidence for restricted fluid migration in 2 GPa eclogites. *J. Metamorph. Geol.* 12, 747–760.
- Gorman, P.J., Kerrick, D.M., Connolly, J.A.D., 2006. Modeling open system metamorphic devolatilization of subducting slabs. *Geochim., Geophys., Geosyst.* 7, 125. doi:10.1029/2005GC001.
- Hanson, R.B., 1997. Hydrodynamics of regional metamorphism due to continental collision. *Econ. Geol.* 92, 880–891.
- Hayba, D.O., Ingebritsen, S.E., 1994. The Computer Model HYDROTHERM, a Three-Dimensional Finite-Difference Model to Simulate Ground-Water Flow and Heat Transport in the Temperature Range of 0 to 1200 degrees Celsius. U.S. Geological Survey Water-Resources Investigations Report 94–4045. 85 pp.
- Holland, T.J.B., Powell, R., 1991. A compensated Redlich-Kwong equation for volumes and fugacities of CO₂ and H₂O in the range 1 bar to 50 kbar and 100–1600 °C. *Contrib. Mineral. Petrol.* 109, 265–273.
- Höpfer, N., Schumacher, J.C., 1977. New field work and interpretations of the sedimentary sequence, the position of the ophiolitic rocks and subsequent deformation on Syros, Cyclades, Greece. *Beih. Eur. J. Mineral.* 9, 162.
- Huenges, E., Erzinger, J., Kuck, J., Engeser, B., Kessels, W., 1997. The permeable crust: geohydraulic properties down to 9101 m depth. *J. Geophys. Res.* 102, 18,255–18,265.
- Ingebritsen, S.E., Manning, C.E., 1999. Geological implications of a permeability–depth curve for the continental crust. *Geology* 27, 1107–1110.
- Kerrick, D.M., Connolly, J.A.D., 2001a. Metamorphic devolatilization of subducted marine sediments and the transport of volatiles into the Earth's mantle. *Nature* 411, 293–296.
- Kerrick, D.M., Connolly, J.A.D., 2001b. Metamorphic devolatilization of subducted oceanic metabasalts: implications for seismicity, arc magmatism, and volatile recycling. *Earth Planet. Sci. Lett.* 189, 19–29.
- King, R.L., Kohn, M.J., Eiler, J.M., 2003. Constraints on the petrologic structure of the slab–mantle interface from Franciscan Complex exotic ultramafic blocks. *Geol. Soc. Amer. Bull.* 115, 1097–1109.
- Manning, C.E., 1997. Coupled reaction and flow in subduction zones: silica metasomatism in the mantle wedge. In: Jamtveit, B., Yardley, B.W.D. (Eds.), *Fluid Flow and Transport in Rocks*. Chapman-Hall, London, pp. 139–148.
- Manning, C.E., Ingebritsen, S.E., 1999. Permeability of the continental crust: implications of geothermal data and metamorphic systems. *Rev. Geophys.* 37, 127–150.
- Marschall, H.R., Ludwig, T., Altherr, R., Kalt, A., Tonarini, S., 2006. Syros metasomatic tourmaline: evidence for very high- $\delta^{11}\text{B}$ fluids in subduction zones. *J. Petrol.* 47. doi:10.1093/petrology/eg1031.
- Matthews, A., 1994. Oxygen isotope geothermometers for metamorphic rocks. *J. Metamorph. Geol.* 12, 211–220.
- Melidonis, N.G., 1980. The geological structure and mineral deposits of Tinos island (Cyclades, Greece). *Geol. Greece* 13, 1–80.
- Okrusch, M., Bröcker, M., 1990. Eclogites associated with high-grade blueschists in the Cyclades archipelago, Greece: a review. *Eur. J. Mineral.* 2, 451–478.
- Oliver, N.H.S., Valenta, R.K., Wall, V.J., 1990. The effect of heterogeneous stress and strain on metamorphic fluid flow, Mary Kathleen, Australia, and a model for large scale fluid circulation. *J. Metamorph. Geol.* 8, 311–332.
- Peacock, S.M., 1990. Fluid processes in subduction zones. *Science* 248, 329–337.
- Philippot, P., Selverstone, J., 1991. Trace-element-rich brines in eclogitic veins: implications for fluid composition and transport during subduction. *Contrib. Mineral. Petrol.* 106, 417–430.
- Putlitz, B., Matthews, A., Valley, J.W., 2000. Oxygen and hydrogen isotope study of high-pressure metagabbros and metabasalts (Cyclades, Greece): implications for the subduction of oceanic crust. *Contrib. Mineral. Petrol.* 138, 114–126.
- Ridley, J., Dixon, J.E., 1984. Reaction pathways during the progressive deformation of a blueschist metabasite: the role of chemical disequilibrium and restricted range equilibrium. *J. Metamorph. Geol.* 2, 115–128.
- Rumble III, D., Spear, F.S., 1983. Oxygen isotope equilibration and permeability enhancement during regional metamorphism. *J. Geol. Soc. (Lond.)* 140, 619628.
- Rye, R.O., Schuiling, R.D., Rye, D.M., Jansen, J.B.H., 1976. Carbon, hydrogen and oxygen isotope studies of the regional metamorphic complex at Naxos, Greece. *Geochim. Cosmochim. Acta* 40, 1031–1049.
- Schliestedt, M., Altherr, R., Matthews, A., 1987. Evolution of the Cycladic crystalline complex: petrology, isotope geochemistry, and geochronology. In: Helgeson, H.C. (Ed.), *Chemical Transport in Metasomatic Processes*. Dordrecht, Reidel, NATO ASI Series. Springer-Verlag, Berlin, pp. 389–428.
- Selverstone, J., Franz, G., Thomas, S., Getty, S., 1992. Fluid variability in 2 GPa eclogites as an indicator of fluid behavior during subduction. *Contrib. Mineral. Petrol.* 112, 341–357.
- Sorensen, S.S., Grossman, J.N., 1989. Enrichment of trace elements in garnet-amphibolites from a paleo-subduction zone: Catalina Schist, Southern California. *Geochim. Cosmochim. Acta* 53, 3155–3177.
- Tomaschek, F., Kennedy, A.K., Villa, I.M., Lagos, M., Ballhaus, C., 2003. Zircon from Syros, Cyclades, Greece—recrystallization and mobilization of zircon during high-pressure metamorphism. *J. Petrol.* 44, 1977–2002.
- Trotet, F., Jolivet, L., Vidal, O., 2001a. Tectono-metamorphic evolution of Syros and Sifnos islands (Cyclades, Greece). *Tectonophysics* 338, 179–206.
- Trotet, F., Vidal, O., Jolivet, L., 2001b. Exhumation of Syros and Sifnos metamorphic rocks (Cyclades, Greece). New constraints on the P–T paths. *Eur. J. Mineral.* 13, 901–920.
- Walder, J., Nur, A., 1984. Porosity reduction and crustal pore pressure development. *J. Geophys. Res.* 89, 11,539–11,548.
- Wong, T., Ko, S., Olgaard, D.L., 1997. Generation and maintenance of pore pressure excess in a dehydrating system: 2. Theoretical analysis. *J. Geophys. Res.* 102, 841–852.